Image watermarking based on scale-space representation

Jin S. Seo and Chang D. Yoo

Department of Electrical Engineering and Computer Science
Korea Advanced Institute of Science and Technology
Daejeon 305-701, Korea

ABSTRACT

This paper proposes a novel method for content-based watermarking based on feature points of an image. At each feature point, watermark is embedded after affine normalization according to the local characteristic scale and orientation. The characteristic scale is the scale at which the normalized scale-space representation of an image attains a maximum value, and the characteristic orientation is the angle of the principal axis of an image. By binding watermarking with the local characteristics of an image, resilience against affine transformations can be obtained. Experimental results show that the proposed method is robust against various image processing steps including affine transformations, cropping, filtering and JPEG compression.

Keywords: watermarking, feature points, scale space, geometric distortion, content-based synchronization

1. INTRODUCTION

With the development of watermarking technologies, attacks against watermarking systems have become more sophisticated. In general, the attacks on watermarking systems can be categorized into noise-like signal processing and geometric distortions. While the noise-like signal processing, such as lossy compression, denoising, noise addition and lowpass filtering, reduces watermark energy, geometric distortions induce synchronization errors between the original and the embedded watermark patterns and therefore can mislead the watermark detector. Most of the previous methods have addressed the robustness problem against noise-like signal processing attacks and only a few specialized watermarking methods have addressed the geometric distortions. These few can be classified into *non-blind scheme*,[1,2] *invariant transform*,[3,4] *embedding-based synchronization*[5,6] and *content-based synchronization*.[7–9]

The proposed method can be classified as the content-based synchronization method. By binding watermark synchronization with image characteristics, watermark detection can be done without synchronization error. More specifically, feature points of an image are used for referencing watermark embedding and detection. Feature points are sufficiently invariant against various image processing steps to be considered as one of the genuine characteristics of an image. There have been approaches that use feature points of an image as a reference for watermarking.[8,9] However, these approaches, which do not consider the variation of feature points regarding to the scaling of an image, have limited robustness against scaling. By using scale-space theory in extracting feature points of an image, we will show that watermark can be adapted to the scale changes. The details of scale space and scale-invariant feature points are described in Section 2. For each scale-invariant feature point, the characteristic orientation is obtained by the principal axes moments.[10] By synchronizing watermark embedding and detection with the characteristic scale and orientation of each feature point, the proposed watermarking method achieves robustness against both the noise-like and the geometric attacks.

This paper is organized as follows. Section 2 describes the scale-space concepts and feature-point detection. Section 3 describes the proposed watermarking method. Section 4 evaluates the performance of the proposed method. Section 5 summarizes the performance and the limitations of the proposed method.

Further author information: (Send correspondence to Jin S. Seo)
Jin S. Seo: jsseo@kaist.ac.kr and Chang D. Yoo: cdyoo@ee.kaist.ac.kr

Security, Steganography, and Watermarking of Multimedia Contents VI, edited by Edward J. Delp III, Ping W. Wong, Proc. of SPIE-IS&T Electronic Imaging, SPIE Vol. 5306 © 2004 SPIE and IS&T · 0277-786X/04/$15

2. FEATURE DETECTION IN SCALE SPACE

To develop a content-based method, image characteristics appropriate for watermarking should be carefully selected. Feature points can be a good candidate for content-based watermarking since there exist feature point detection methods that are proven to be robust against many image processing steps such as sharpening, blurring, compression and geometric transformations.[11–13] For this reason, we have chosen feature points for watermark synchronization.

2.1. Scale space and automatic scale selection

Detection of feature points, which are invariant to geometric transformations, has been one of the main issues in pattern recognition and computer vision. This leads to the study of scale space and automatic scale selection of an image. The scale-space representation is a set of images represented at different levels of resolutions.[11] More precisely linear scale-space representation $L : \mathbb{R}^2 \times \mathbb{R}_+ \rightarrow \mathbb{R}$ of an image $f : \mathbb{R}^2 \rightarrow \mathbb{R}$ is defined as the solution to the diffusion equation

$$\partial_s L(\mathbf{x}; s) = \frac{1}{2}\nabla^T \nabla L(\mathbf{x}; s) = \frac{1}{2}\mathrm{div}(\nabla L(\mathbf{x}; s)) \tag{1}$$

with the initial condition $L(\mathbf{x}; 0) = f(\mathbf{x})$ where $\mathbf{x} = (x, y)$ refers to the image spatial coordinate and $\partial_s L(\mathbf{x}; s) = \frac{\partial}{\partial_s} L(\mathbf{x}; s)$. As a solution to the above equation, given a scale s, the *uniform Gaussian scale-space representation*[14] is defined by

$$L(\mathbf{x}; s) = g(\mathbf{x}; s) * f(\mathbf{x}) \tag{2}$$

where $g(\mathbf{x}; s)$ is the associated uniform Gaussian kernel with standard deviation s and mean zero. A well-known property of the scale-space representation is that the amplitude of spatial derivatives in general *decreases with scale*,[11] i.e. if a signal is subjected to scale-space smoothing, then the numerical values of spatial derivatives computed from the smoothed data can be expected to decrease. Thus to select scale that reflects local characteristics of an image, a scale-normalized derivative ∂^N is introduced[11] as follows:

$$\partial^N_{x^{\alpha_1}, y^{\alpha_2}} = s^{\alpha_1+\alpha_2} \partial_{x^{\alpha_1}} \partial_{y^{\alpha_2}} \tag{3}$$

where α_1 and α_2 are the order of differentiation. To give a formal characterization of the scaling property, consider two images f and $\tilde{f}$ related by $f(x) = \tilde{f}(tx)$. The scale-space representations L and $\tilde{L}$ of f and $\tilde{f}$ are defined by equation (2) respectively. Then the scale-space representations is related by

$$L(\mathbf{x}; s) = \tilde{L}(\tilde{\mathbf{x}}; \tilde{s}) \tag{4}$$

where $\tilde{\mathbf{x}} = t\mathbf{x}$ and $\tilde{s} = ts$. Differentiation of equation (4) by x and y with order α_1 and α_2 gives the following relationship:

$$\partial_{x^{\alpha_1}} \partial_{y^{\alpha_2}} L(\mathbf{x}; s) = t^{\alpha_1+\alpha_2} \partial_{\tilde{x}^{\alpha_1}} \partial_{\tilde{y}^{\alpha_2}} \tilde{L}(\tilde{\mathbf{x}}; \tilde{s}). \tag{5}$$

By multiplying $s^{\alpha_1+\alpha_2}$ to equation (5), we can obtain the *scale invariance* from equation (3) as follows:

$$\partial^N_{x^{\alpha_1}, y^{\alpha_2}} L(\mathbf{x}; s) = \partial^N_{\tilde{x}^{\alpha_1}, \tilde{y}^{\alpha_2}} \tilde{L}(\tilde{\mathbf{x}}; \tilde{s}). \tag{6}$$

The scale level, at which a combination of normalized derivatives attains a local maximum over scales, can be treated as reflecting a characteristic length of corresponding structure. Thus the normalized scale-space maxima have been considered as *characteristic scale* of the image. The scale-invariance property of normalized derivatives ensures the invariance of scale-space maxima.[11] If a normalized scale-space maximum is at $(\mathbf{x_0}; s_0)$ in the scale-space representation of an image f, then the corresponding scale-space maximum is assumed at $(t\mathbf{x_0}; ts_0)$ in the scale-space representation of $\tilde{f}$. Fig. 1 shows an example of scale selection. For the same point in the original and the cropped and scaled image (scale factor is 2.0), we compute the amplitude of normalized derivatives (Laplacian)[15] over scales. The figure shows that the characteristic scale is relatively invariant to scaling. The ratio of the scales at corresponding points in the two images, at which the maxima were found, is equal to the scale factor between the two images.

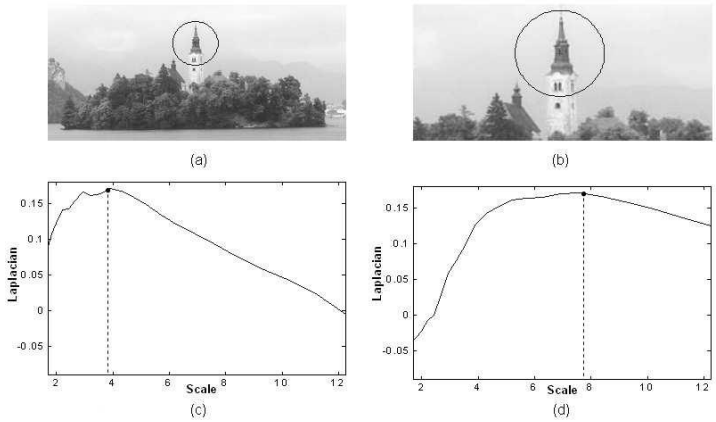

Figure 1. (a) Original image, (b) 50% cropped and 200% scaled image, (c) scale-normalized Laplacian of the image (a) around the feature point at the center of disk, (d) scale-normalized Laplacian of the image (b) around the feature point at the center of disk; the radius of the circle is 10σ where σ is the characteristic scale at that point.

2.2. Detection of scale invariant feature points

Any suitable scale-space feature point detector can be used for the proposed watermarking method. In this paper, we use the *Harris-Laplacian* method.[12] Scale-invariant feature points are detected based on the scale selection at Harris corner points. The Harris-Laplacian method first builds a scale-space representation for the Harris corner strength measure. The scale-normalized second-moment matrix $U(\mathbf{x}, s)$ is given by

$$U(\mathbf{x}, s) = s^2 g(\mathbf{x}; s) * \begin{bmatrix} L_x^2(\mathbf{x}; t) & L_x L_y(\mathbf{x}; t) \\ L_x L_y(\mathbf{x}; t) & L_y^2(\mathbf{x}; t) \end{bmatrix} \tag{7}$$

where $L_x = \partial_x L(\mathbf{x}; s)$ and t is set to $\frac{s}{2}$ in this paper. The Harris corner strength measure $H(\mathbf{x}, s_n)$ at scale s_n and point $\mathbf{x}$ is given by a second moment matrix $U(\mathbf{x}, s_n)$ as follows:

$$H(\mathbf{x}, s_n) = \det U(\mathbf{x}, s_n) - 0.04 * (\text{trace } U(\mathbf{x}, s_n))^2. \tag{8}$$

At each level of the scale space, corner points are detected as the local maxima in the image plane as follows:

$$\begin{gathered} H(\mathbf{x}, s_n) > H(\mathbf{x_w}, s_n) \;\; \forall \, \mathbf{x_w} \in W \\ H(\mathbf{x}, s_n) > t_h \end{gathered} \tag{9}$$

where W and t_h denotes the neighborhood of the point $\mathbf{x}$ and the detection threshold respectively. Among the corner points we select the points at which a local Laplacian operator is maximal over scales. The scale-normalized Laplacian of an image $J(\mathbf{x}, s_n)$ at scale s_n and point $\mathbf{x}$ is given by

$$J(\mathbf{x}, s_n) = |s_n^2 (L_{xx}(\mathbf{x}, s_n) + L_{yy}(\mathbf{x}, s_n))|. \tag{10}$$

For each Harris maximum point, we check whether its Laplacian is a maximum at the scale s_n or not by the following condition:

$$\begin{gathered} (J(\mathbf{x}, s_n) > J(\mathbf{x}, s_{n-1})) \cap (J(\mathbf{x}, s_n) > J(\mathbf{x}, s_{n+1})) \\ J(\mathbf{x}, s_n) > t_l \end{gathered} \tag{11}$$

where t_l denotes the detection threshold. Thus the scale-invariant feature points are determined by satisfying both equations (9) and (11). By using two measures, the feature points are characteristic to both the image plane and the scale dimension. Moreover, the characteristic scale information is automatically obtained during feature-point extraction. In the comparative tests,[12,13] the Harris corner points proved to be the most reliable under various image processing steps, and the Laplacian was determined to have the best repeatability of scale selection under large scale changes. The scale-invariant feature points selected by this method exhibit invariance to scale, rotation and translation as well as robustness to illumination changes.[12]

3. PROPOSED WATERMARKING SCHEME

Content-based watermarking schemes utilize the fact that the features of content can afford a reference invariant to geometric distortions. This idea has also been exploited for invariant pattern recognition and image retrieval.[12, 16, 17] In this paper, we apply the same idea to watermark synchronization. Watermark is shaped adaptively using the characteristic scale and orientation of the feature point. By using local characteristics of an image, the proposed method achieves both locality and affine resilience.

3.1. Watermark embedding

We extract feature points of the scale-space representation of an image appropriate for watermarking. In equation (8), the determinant and the trace of the scale-normalized second-moment matrix $U(\mathbf{x}, s)$[11, 16] are used in calculating $H(\mathbf{x}, s)$. This means that corner strengths can be compared across different scales using the value of the *scale-normalized Harris corner strength* (SHCS) measure $H(\mathbf{x}, s)$. By assuming that the feature point with larger SHCS measure is more likely to be repeatable, the feature points with the locally largest SHCS measure are considered for watermarking. Fig. 2(a) shows the detected feature points for Lena image. Since the watermarked image can be scaled up or down, we first consider the feature points with characteristic scale σ_c in the middle-scale band ($5 \leq \sigma_c \leq 10$). Fig. 2(b) and (c) show the feature points with characteristic scale in the middle-scale and the low-scale ($3.5 < \sigma_c < 5$) and high-scale ($10 < \sigma_c < 12.5$) bands respectively. It is assumed that each feature point represents a disk with radius $R_c = 8\sigma_c$. If a number of disks are overlapping, the SHCS measures of the feature points are compared, and the one with the largest SHCS measure survives and the others are erased. By repeating the same process for all the feature points with characteristic scale in the middle-scale band, we can select feature points that has the largest SHCS measure in their neighborhood. While retaining the selected feature points with characteristic scale in the middle-scale band, the same process is performed for the feature points with characteristic scale in the high-scale and the low-scale band respectively. In other words, if the disks of feature points with characteristic scale in the low-scale and the high-scale band are overlapped with the disks of the selected feature points with characteristic scale in the middle-scale band, they are erased. Otherwise, the same selection process, which is used in the feature points with characteristic scale in the middle-scale band, is applied to the feature points with characteristic scale in the low-scale and the high-scale band respectively. Fig. 2(d) shows the feature points that survive after all. The watermark is embedded additively inside the disks in Fig. 2(d).

After selecting feature points for watermarking, the characteristic orientation can be decided by the *principal axes* moments.[10] On each selected disk, the moments μ_{pq} with origin at the center of the disk (x_c, y_c) are defined as follows:

$$\mu_{pq} = \int_{-\infty}^{\infty}\int_{-\infty}^{\infty}(x - x_c)^p(y - y_c)^q f(x, y)C(x - x_c, y - y_c)dxdy \quad \text{for } p, q = 0, 1, 2, \cdots \tag{12}$$

where

$$C(x, y) = \begin{cases} 1 & \text{if } \sqrt{x^2 + y^2} \leq R_c \\ 0 & \text{otherwise} \end{cases} \tag{13}$$

After rotating the disk by an angle θ, the moments μ'_{pq} is given as follows[10]:

$$\begin{aligned}\mu'_{pq} = &\sum_{r=0}^{p}\sum_{s=0}^{q}\binom{p}{r}\binom{q}{s}(\cos\theta)^{p-r+s} \\ &\cdot(\sin\theta)^{q+r-s}\mu_{p+q-r-s,r+s}.\end{aligned} \tag{14}$$

The principal axis is obtained by rotating the axis of the moments until μ'_{11} is zero. The characteristic orientation θ_c, measured from the original axis, is defined by

$$\tan 2\theta_c = \frac{2\mu_{11}}{\mu_{20} - \mu_{02}}. \tag{15}$$

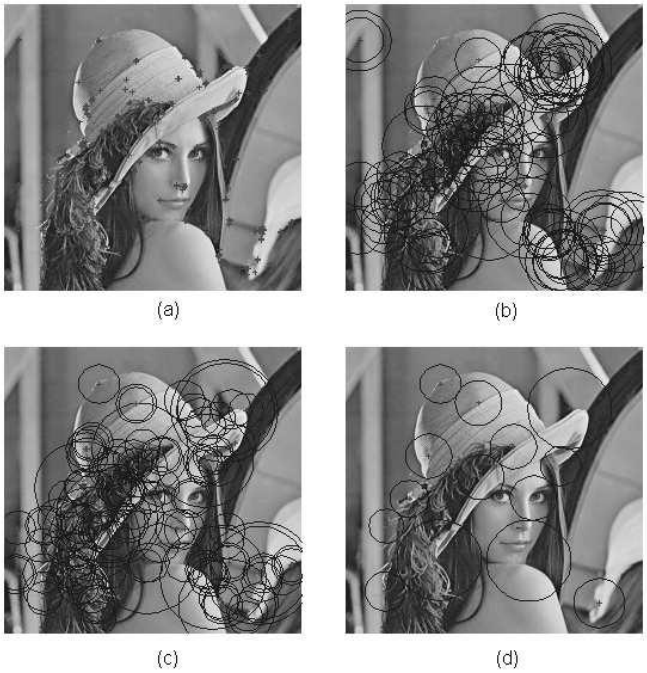

Figure 2. Feature points (a) detected (b) with characteristic scale in the middle-scale band (c) with characteristic scale in the low-scale and high-scale bands (d) finally selected; the radius of each circle is 8σ where σ is the characteristic scale at that point.

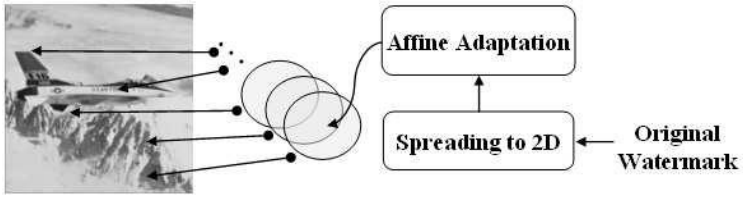

Figure 3: Watermark embedding based on feature points

The angle θ_c obtained by equation (15) may be with respect to either the major principal axis or the minor principal axis. The correct orientation will be $\theta_c + n\pi/2$ where an integer n is needed to be determined by additional constraints. The additional constraints can be $\mu'_{20} > 0$ and $\mu'_{30} > 0$. The determined orientation is used as a characteristic orientation of the disk. The details of the principal axes moments can be found in the paper.[10]

The proposed watermark embedding method is shown in Fig. 3. The construction of a prototype circular watermark is shown in Fig. 4. A binary zero-mean pseudo random sequence $B = (b_1, b_2, \ldots, b_M)$ is generated by a secure key and spread over the first quadrant. The quadrant is rotated and copied into the other quadrants. Then, the prototype watermark pattern W with a support inside a circle (radius R_o) is obtained. In spatial domain, the prototype watermark is embedded after scaling and rotation according to the characteristic scale σ_c ($R_c = 8\sigma_c$) and orientation θ_c at each selected feature point $\mathbf{x_c}$. Mathematically it can be written as follows:

$$f'(\mathbf{x}) = f(\mathbf{x}) + \alpha(\mathbf{x}) W(\Pi_{R_c,\theta_c}(\mathbf{x} - \mathbf{x_c})^T) \tag{16}$$

where $\alpha(\mathbf{x})$ is the local masking function calculated from the Human Visual System (HVS)[18] to make the

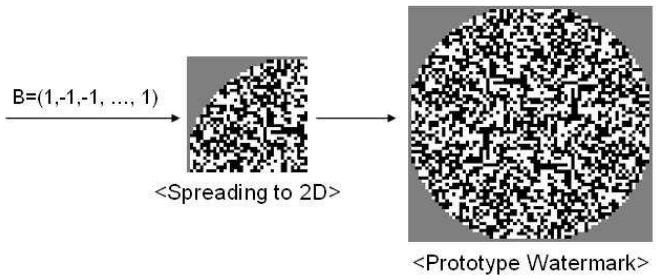

Figure 4. Construction of prototype watermark from one-dimensional binary random sequence; white, gray and black refer to 1, 0 and -1 respectively.

embedded watermark imperceptible, and the affine matrix Π_{R_c,θ_c} is given by

$$\Pi_{R_c,\theta_c} = \frac{R_o}{R_c} \begin{bmatrix} \cos\theta_c & -\sin\theta_c \\ \sin\theta_c & \cos\theta_c \end{bmatrix} \tag{17}$$

The watermark embedding procedure is summarized as follows:

1. Extract feature points of scale-space representation of an image as shown in Fig. 2(a).
2. Considering the spatial positions, SHCS measures and characteristic scales of the extracted feature points, final feature points for watermarking are selected as shown in Fig. 2(d).
3. At each selected feature point, the characteristic orientation of the disk is calculated from the principal axes moments.
4. The watermark is embedded additively into the selected disks of the image after adapting to the characteristic scale and orientation at each feature point as shown in Fig. 3.

3.2. Watermark detection

The proposed watermark detection method is shown in Fig. 5. It is assumed that watermark exists at the feature points with the locally largest SHCS measure as the watermark was embedded. After extracting feature points from an image, the same feature-point selection process used in the watermark embedding is performed. Since the selection process after the watermark embedding and attacks may not be repeatable, the feature-point selection process is iteratively performed after erasing the already selected points until the N points are selected (typically $N = 50$). At each selected feature point x_c, the detection mask D is obtained by scale and orientation normalization according to the characteristic scale and orientation as follows:

$$D = f_w(\Pi^{-1}_{R_c,\theta_c}(\mathbf{x} - \mathbf{x_c})^T) \tag{18}$$

where f_w is the estimated watermark from an image by using Wiener filter.[8] The four quadrants of D are added and then dispread into the sequence $P = (p_1, p_2, \ldots, p_M)$. Watermark detection is based on normalized correlation[19] between the original watermark B and the estimated watermark P as follows:

$$Z = \frac{B \cdot \tilde{P}}{\sqrt{(B \cdot B)(\tilde{P} \cdot \tilde{P})}} \tag{19}$$

where $\tilde{P} = (p_1 - \bar{p}, p_2 - \bar{p}, \ldots, p_M - \bar{p})$, $\bar{p}$ is the mean value of P and $B \cdot \tilde{P} = \sum_{i=1}^{M} b_i \tilde{p}_i$. Using the normalized correlation Z, the watermark detection problem could be formulated as the following hypothesis testing:

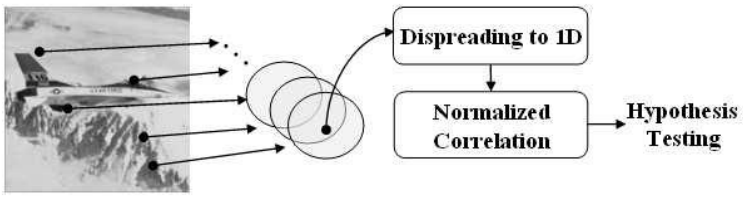

Figure 5: Watermark detection based on feature points

- H_0: An image is watermarked by B if $Z \geq T$
- H_1: An image is not watermarked by B if $Z < T$.

where T is the watermark detection threshold. We will discuss how to determine the threshold T in Section 4.1.

The watermark detection procedure is summarized as follows:

1. Extract feature points of scale-space representation of an image.
2. Find N most probably watermarked candidate feature points across the scale space.
3. At each candidate feature point, the characteristic orientation is obtained by the principal axes moments.
4. Normalized correlation detector is applied to each candidate disk after adapting the disk to the characteristic orientation.
5. According to the detection results, we finally make a decision whether the image is watermarked or not by testing hypothesis with the threshold T.

4. EXPERIMENTAL RESULTS

In the experiments, we have used scale-space representation with 36 scale levels, $M = 1024$ and $R_o = 36$. The scale-space representation starts with an initial scale of 2.3 and the scale factor between two levels of resolution is 1.05. Since watermark pattern is pseudo randomly generated, watermark correlation detector is highly sensitive to the synchronization errors. The pseudo random watermark pattern showed vulnerability to geometric distortions more than $0.01R_c$ pixel translation, 1.5% scaling and 0.75 degree of rotation. However, the feature point detector can not have such a high accuracy since we deal with sampled spatial (digital images) and scale spaces. Most of the detected feature points typically show deviation up to the amount of 1.5 pixel of the location, 5% of the characteristic scale and 3 degree of characteristic orientation after various attacks. To resolve this mismatch, we performed correlation detection by changing position, scale and orientation of a candidate disk K times. We call this process *local search*. In the experiments, the local search is performed by changing the position, the characteristic scale and orientation of each feature point in the amount of $\pm 0.02R_c$ pixel, $\pm 0.025\sigma_c$ and ± 1.5 degree respectively. Then local search space amounts to 81 (3 in x and y direction, characteristic scale and orientation respectively) for each feature point.

4.1. False alarm analysis

To determine the watermark detection threshold T, the false alarm rate P_{FA} and the false rejection rate P_{FR} should be considered. The false alarm rate P_{FA} is the probability to declare an unmarked image as *marked*. The false rejection rate P_{FR} is the probability to declare a marked image as *unmarked*. There is a tradeoff between the two probabilities in selecting threshold T. In practice P_{FR} is difficult to analyze since there are plenty of image processing steps of those we do not know the exact characteristics. Thus it is common to select a threshold T of minimizing P_{FR} subject to a fixed P_{FA}. First we examine the false alarm rate of each disk. By

Table 1: Threshold T of correlation detector for $P_{FA-\text{image}}$ with settings $M = 1024$, $K = 81$ and $N = 50$

$P_{FA-\text{image}}$	$\mu = 1$	$\mu = 2$	$\mu = 3$
10^{-4}	0.1704	0.1405	0.1276
10^{-5}	0.1827	0.1479	0.1331
10^{-6}	0.1945	0.1550	0.1385
10^{-7}	0.2054	0.1618	0.1437

assuming that the watermark has zero mean and unit variance and is independent with the image, the mean $\bar{Z}$ and the standard deviation σ_Z of normalized correlation Z for unmarked images are given by[19]

$$\bar{Z} = 0, \quad \sigma_Z = \frac{1}{\sqrt{M}}. \tag{20}$$

By the Gaussian assumption of Z, the false alarm rate of the correlation output $P_{FA-\text{cor}}$ is given for a certain value of the threshold T as follows:

$$P_{FA-\text{cor}} = \int_T^\infty \frac{\sqrt{M}}{\sqrt{2\pi}} \exp\Big[\frac{-x^2 M}{2}\Big] dx = \frac{1}{2}\text{erfc}\Big(\frac{\sqrt{M}T}{\sqrt{2}}\Big). \tag{21}$$

To compensate for the inaccuracy of the position, the characteristic scale and orientation of the feature point after attacks, the correlation detection is performed at each feature point K times (*local search*, in our case $K = 81$). Then the false alarm rate of each disk $P_{FA-\text{disk}}$ is given by

$$P_{FA-\text{disk}} = \sum_{i=1}^{K} \binom{K}{i} P_{FA-\text{cor}}^i \Big(1 - P_{FA-\text{cor}}\Big)^{(K-i)} \tag{22}$$

$$= 1 - (1 - P_{FA-\text{cor}})^K. \tag{23}$$

By viewing all the watermarked disks as independent communication channels, we claim the existence of watermark if the same watermark is detected from at least μ number of disks.[9] Then the false alarm probability for an image $P_{FA-\text{image}}$ is given by

$$P_{FA-\text{image}} = \sum_{i=\mu}^{N} \binom{N}{i} P_{FA-\text{disk}}^i \Big(1 - P_{FA-\text{disk}}\Big)^{(N-i)} \tag{24}$$

where N is the number of disks used in the watermark detection. In our case, we choose 50 most probably watermarked candidate feature points based on SHCS measure through the scale space as in the watermark embedding and try to detect watermark. Table 1 shows the watermark detection threshold with the settings $M = 1024$, $K = 81$ and $N = 50$ for $\mu = 1, 2, 3$. All the tests in Section 4.2 are done with the threshold at $P_{FA-\text{image}} = 10^{-5}$.

4.2. Robustness test

The proposed watermarking scheme is tested on the four popular test images: 512×512 Airplane, Lena, Baboon and Peppers. Original watermark pattern B is prepared as a zero-mean pseudo-random 1024-length pattern and spread into the disk with the radius $R_o = 36$. The PSNR of watermarked image was 42.86, 44.66, 38.30 and 43.96 dB for Airplane, Lena, Baboon and Peppers respectively. To test the robustness of the proposed method, all the watermarked images were subjected to various kinds of image processing steps.[20] For the experiments, we choose $P_{FA-\text{image}} = 10^{-5}$. Watermark detection results for common signal processing steps and geometric distortions are shown in Table 2 and 3 respectively. Three numbers in the Tables indicate the

Table 2. Watermark detection results under non-geometric signal processing steps. Three numbers in the Tables indicate the number of detected disks for $\mu = 1, 2, 3$ respectively. The number of watermarked disks are 14 for Airplane, Lena and Peppers and 22 for Baboon.

Processing	**AIR**	**LENA**	**BAB**	**PEP**
Gaussian filter	8, 8, 8	12, 12, 12	5, 8, 9	11, 11, 11
Sharpening filter	6, 6, 6	9, 9, 9	3, 3, 3	6, 6, 6
Median filter (4×4)	5, 5, 5	9, 9, 9	2, 3, 3	10, 10, 10
Additive uniform noise (scale=0.1)	7, 7, 7	10, 10, 10	4, 4, 4	10, 10, 10
Additive uniform noise (scale=0.2)	7, 7, 7	6, 6, 6	2, 2, 2	5, 5, 6
Histogram equalization	0, 0, 0	3, 4, 4	2, 2, 3	4, 5, 5
JPEG (Q=70%)	11, 11, 11	10, 10, 10	9, 9, 10	10, 10, 10
JPEG (Q=60%)	11, 12, 12	8, 9, 9	6, 6, 6	13, 13, 13
JPEG (Q=50%)	10, 11, 11	8, 11, 11	5, 6, 6	12, 12, 12
JPEG (Q=40%)	6, 7, 8	6, 7, 8	4, 4, 5	8, 9, 9
JPEG (Q=30%)	5, 8, 9	4, 7, 8	2, 3, 3	5, 11, 12
Gaussian filter + JPEG (Q=90%)	9, 9, 9	8, 10, 10	2, 5, 7	11, 11, 11
Sharpening filter + JPEG (Q=90%)	6, 6, 6	9, 9, 9	2, 2, 2	6, 6, 6
Median filter + JPEG (Q=90%)	6, 6, 6	8, 9, 9	2, 3, 3	10, 10, 10
FMLR	1, 1, 1	0, 2, 2	8, 8, 8	4, 7, 7

number of detected disks for $\mu = 1, 2, 3$ respectively. The results denote that the proposed method is robust against affine transformations, which preserve aspect ratio, local geometric attacks (such as random bending attack), and other image processing steps including compression and various filtering. In fact the watermark detection performance strongly depends on the location and the image characteristics of the watermarked disks. If a disk is located in the border of an image, it might be removed after cropping. The watermarked disks in the textured area are less robust since many new feature points may show up, and the feature points of the watermarked disks may shift considerably (more than 1 pixel) after either geometric distortions or noise-like signal processing attacks.[8,9] The feature points in the intersection of strong edges show best repeatability. These facts are reflected in Table 2 and 3, and the textured image Baboon showed less robustness than the other images.

5. CONCLUSION

This paper shows that resilience against geometric distortions in watermark detection can be significantly improved by using the synchronization based on feature points. The robustness against geometric distortions is essential because it is quite easy to impose geometric distortions to images with modern computers. Watermark is embedded into an image at each selected feature point after adapting to the local characteristic scale and orientation. Invariance of watermark against translation, scaling and rotation is obtained by the feature points, characteristic scale and orientation respectively. The original image is not needed in the watermark detector. Two limitations are commonly quoted on the content-based watermarking methods: the inaccuracy of feature point detector[8,9] and the added computational complexity. In this paper, the inaccuracy was overcome by using the local search. Obviously the proposed method is computationally more demanding than watermarking methods that do not handle geometric distortions. However, it is certainly less burdensome than exhaustive search. The experimental results show that the robustness of the proposed content-based watermarking method, especially to scaling and cropping, is improved by using scale-space feature points. This implies that there may be room for improvement of watermarking performance by using refined pattern recognition techniques. Future work includes the development of more robust feature point detector, especially on textured areas, and watermarking method that is adaptable to nonisometric geometric distortions.

Table 3. Watermark detection results under geometric signal processing steps. Three numbers in the Tables indicate the number of detected disks for $\mu = 1, 2, 3$ respectively. The number of watermarked disks are 14 for Airplane, Lena and Peppers and 22 for Baboon. Note that autocrop refers to cropping to original size after rotation.

Processing	**AIR**	**LENA**	**BAB**	**PEP**
17 column 5 row removed	7, 7, 7	8, 8, 8	3, 6, 6	10, 10, 10
Cropping 15% off	5, 5, 5	6, 6, 6	6, 6, 6	2, 2, 2
Cropping 25% off	1, 1, 1	3, 3, 3	5, 5, 5	3, 3, 3
Rotation 20° + autocrop	4, 4, 4	8, 8, 8	5, 6, 6	4, 4, 4
Rotation 45° + autocrop	5, 5, 5	5, 6, 6	2, 2, 2	4, 4, 4
Scaling 90%	3, 3, 3	3, 3, 3	1, 3, 3	4, 5, 5
Scaling 75%	4, 4, 4	2, 2, 2	1, 1, 1	5, 5, 5
Scaling 50%	0, 1, 2	2, 3, 3	0, 0, 1	2, 4, 4
Shearing (1%)	3, 3, 3	6, 6, 6	4, 5, 5	11, 11, 11
Shearing (5%)	4, 5, 5	1, 4, 5	0, 0, 1	0, 2, 3
Linear geometric transform (1.007,0.010,0.010,1.012)	3, 3, 3	6, 6, 6	7, 7, 7	11, 11, 11
Linear geometric transform (1.010,0.013,0.009,1.011)	4, 4, 5	5, 5, 5	10, 10, 10	6, 6, 7
Linear geometric transform (1.013,0.008,0.011,1.008)	7, 7, 7	5, 5, 6	6, 7, 7	10, 10, 10
Random bending attack	6, 7, 7	7, 7, 7	3, 6, 6	6, 8, 8

ACKNOWLEDGMENTS

This work was supported by grant No. R01-2003-000-10829-0 from the Basic Research Program of the Korea Science & Engineering Foundation.

REFERENCES

1. F. Davoine, "Triangular meshes: a solution to resist to geometric distortions based watermark-removal softwares," in *Proc. European Signal Processing Conf.*, 2000.
2. P. Dong, J. Brankov, N. Galatsanos, and Y. Yang, "Geometric robust watermarking based on a new mesh model correction approach," in *Proc. IEEE Int. Conf. Image Processing*, 2002.
3. J. Ruanaidh and T. Pun, "Rotation, scale and translation invariant spread spectrum digital image watermarking," *Signal Process.* **66**, 1998.
4. C.-Y. Lin, M. Wu, J. Bloom, M. Miller, I. Cox, and Y.-M. Lui, "Rotation, scale, and translation resilient public watermarking for images," *IEEE Trans. Image Processing* **10**, 2001.
5. S. Pereira and T. Pun, "Robust template matching for affine resistant image watermarks," *IEEE Trans. Image Processing* **9**, 2000.
6. M. Kutter, "Watermarking resisting to translation, rotation and scaling," in *Int. Symp. on Voice, Video, and Data communication*, *Proc. SPIE* **3528**, 1998.
7. M. Alghoniemy and A. Tewfik, "Geometric distortion correction through image normalization," *Proc. IEEE Int. Conf. Multimedia and Expo*, 2000.
8. P. Bas, J.-M. Chassery, and B. Macq, "Geometrically invariant watermarking using feature points," *IEEE Trans. Image Processing* **11**, 2002.
9. C.-W. Tang and H.-M. Hang, "A feature-based robust digital image watermarking scheme," *IEEE Trans. Signal Processing* **51**, 2003.

10. A. Reeves, R. Prokop, S. Andrews, and F. Kuhl, "Three-dimensional shape analysis using moments and Fourier descriptors," *IEEE Trans. Pattern Anal. and Machine Intell.* **10**, 1988.
11. T. Lindeberg, "Feature detection with automatic scale selection," *Internal Journal of Computer Vision* **30**, 1998.
12. K. Mikolajczyk and C. Schmid, "Indexing based on scale invariant interest points," *Proc. Int. Conf. Computer Vision*, 2001.
13. C. Schmid, R. Mohr, and C. Baukhage, "Comparing and evaluating interest points," *Proc. Int. Conf. Computer Vision*, 1998.
14. J. Babaud, A. Witkin, M. Baudin, and R. Duda, "Uniqueness of the gaussian kernel for scale-space filtering," *IEEE Trans. on Pattern Anal. Machine Intell.* **8**, 1986.
15. A. Jain, *Fundamentals of Digital Image Processing*, Prentice Hall, 1989.
16. A. Baumberg, "Reliable feature matching across widely separated views," *Proc. Computer Vision and Pattern Recognition*, 2000.
17. C. Schmid and R. Mohr, "Local gray value invariants for image retrieval," *IEEE Trans. Pattern Anal. and Machine Intell.* **19**, 1997.
18. B. Girod, "The information theoretical significance of spatial and temporal masking in video signals," *Proc. SPIE/SPSE Conf. on Human Vision, Visual Processing and Digital Display*, 1989.
19. I. Cox, M. Miller, and J. Bloom, *Digital watermarking*, Morgan Kaufmann, 2002.
20. F. Fetitcolas, "Watermarking schemes evaluation," *IEEE Signal procssing Mag.* **17**, 2000.